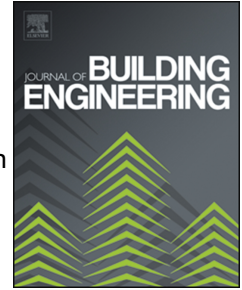


Journal Pre-proof

Performance evaluation of structures with reinforced concrete columns retrofitted with steel jacketing

Sergio Villar-Salinas, Andrés Guzmán, Julián Carrillo



PII: S2352-7102(19)32798-6

DOI: <https://doi.org/10.1016/j.jobe.2020.101510>

Reference: JOBE 101510

To appear in: *Journal of Building Engineering*

Received Date: 10 December 2019

Revised Date: 7 April 2020

Accepted Date: 16 May 2020

Please cite this article as: S. Villar-Salinas, André. Guzmán, Juliá. Carrillo, Performance evaluation of structures with reinforced concrete columns retrofitted with steel jacketing, *Journal of Building Engineering* (2020), doi: <https://doi.org/10.1016/j.jobe.2020.101510>.

This is a PDF file of an article that has undergone enhancements after acceptance, such as the addition of a cover page and metadata, and formatting for readability, but it is not yet the definitive version of record. This version will undergo additional copyediting, typesetting and review before it is published in its final form, but we are providing this version to give early visibility of the article. Please note that, during the production process, errors may be discovered which could affect the content, and all legal disclaimers that apply to the journal pertain.

© 2020 Published by Elsevier Ltd.

Cartagena, Monday, April 6, 2020

Dr.

James M. LaFave, PE

Receiving Editor

Journal of Building Engineering

Ref.: JOBE_2019_2780 (Revision requested on February 8th, 2020)

Performance evaluation of structures considering reinforced concrete columns retrofitted with steel jacketing. **Credit Author Statement**

Dear Editor,

We share an accurate and detailed description of our contributions to the paper referenced in the subject:

Villar-Salinas, Sergio: Conceptualization, methodology, investigation, visualization, supervision and writing – original draft.

Guzmán, Andrés: writing – original draft, resources, writing – review and editing, and visualization.

Carrillo, Julián: writing – review and editing, resources and visualization.

Sincerely yours,



Sergio Villar S.
cc. 93194496 d/9na

Sergio Villar Salinas, MSc

Professor

Department of Civil and Environmental Engineering

Universidad Tecnológica de Bolívar

Campus Tecnológico km 1. Vía Turbaco

Cartagena de Indias, BOL, Colombia 130010

svillars@utb.edu.co

www.utb.edu.co

Phone: [57] 3008038640

Performance evaluation of structures with reinforced concrete columns retrofitted with steel jacketing

Sergio Villar-Salinas^{a*} <https://orcid.org/0000-0002-2320-9822>

Andrés Guzmán^b <https://orcid.org/0000-0003-2472-1390>

Julián Carrillo^c <https://orcid.org/0000-0002-8274-5414>

^a Department of Civil and Environmental Engineering, Universidad Tecnológica de Bolívar, Campus Tecnológico km 1 Vía Turbaco, 130011, Cartagena de Indias, Colombia. E-mail: svillars@utb.edu.co

^b Department of Civil and Environmental Engineering, Universidad del Norte, km 5 Vía Puerto Colombia, Área Metropolitana de Barranquilla, 081007, Barranquilla, Atlántico, Colombia. E-mail: faguzman@uninorte.edu.co

^c Department of Civil Engineering, Universidad Militar Nueva Granada, Carrera 11 No. 101-80, Edificio F, Piso 2, 49300, Bogotá D.C., Colombia. E-mail: julian.carrillo@unimilitar.edu.co

* Corresponding author

Abstract

Several existing reinforced concrete (RC) buildings fail to conform with current seismic codes, increasing its susceptibility to damage and collapse during earthquakes. A concern for building upgrading and rehabilitation has grown considerably in the last decades. However, there is limited information related to the seismic performance of RC buildings retrofitted with steel jacketing. Retrofitting of RC buildings leads to different techniques that have been developed in the last decades. The selection of adequate techniques commonly depends on desired performance levels, financial criteria, or other non-technical judgment. This paper assesses the seismic performance of a six-story RC building retrofitted with steel jacketing that is located in Cartagena de Indias (Colombia). The building was designed and constructed in 2010 without considering the requirements prescribed by the NSR-10 Colombian code. In 2017, another building collapsed in the same city for several non-compliances with Colombian seismic code. This investigation focuses on the seismic upgrading of the building, studying the influence of different material properties of the existing building and load scenarios on the building behavior. The proposed steel jacketing improves the compressive and flexural capacity of retrofitted columns, along with the ductility of the building.

Keywords

Seismic performance, seismic retrofitting, RC buildings, nonlinear modeling, steel jacketing

1 INTRODUCTION

Several existing reinforced concrete (RC) buildings do not conform to current seismic codes, even in regions of high seismic hazard. Therefore, many of these buildings are susceptible to damage and even collapse during earthquakes [1,2]. Structural and non-structural damages and poor performance of RC buildings with code non-compliances have been observed after recent earthquakes [3]. Most of these damages have been evidenced in RC columns with insufficient axial/shear loads capacity given by inadequate longitudinal/transversal reinforcement and dimensions, 90-degree hooks for stirrups at both ends of columns, inadequate detailing in beam-column joint regions, strong-beam and weak-columns, soft stories, weak stories, and poor quality construction [4,5].

The concern for seismic upgrading and rehabilitation has grown in the last decades [2,6,7] following structural and non-structural earthquake-induced damages observed after relevant seismic events in

45 different parts of the world like Northridge (1994), Kobe (1995), Kocaeli (1999), Sichuan (2008), Chile
46 (2010), Ecuador (2016) or Mexico (2017). In Colombia, the government adopted the earthquake-resistant
47 Code for construction in Colombia NSR-10 [8]. This code prescribes criteria and minimum requirements for
48 the design, construction, and technical supervision of new buildings. Also, the code offers design and
49 revision guidelines for those buildings indispensable after an earthquake.

50 Buildings designed according to NSR-10 should be able to resist service loads and low-intensity
51 earthquakes without damage; moderate earthquakes without structural damage, but possibly with some
52 damage in non-structural elements; and strong earthquakes with damage of structural and non-structural
53 elements, but without collapse [9]. Most of the earthquake-resistant codes, including the NSR-10 Colombian
54 Code, establish general requirements for the assessment, upgrade, rehabilitation/retrofitting, and repairing
55 of structural systems after an earthquake, and pre-existing buildings. Nevertheless, further research on the
56 seismic performance of retrofitted RC buildings is needed. Although concerns related to seismic upgrading
57 and retrofitting has increased considerably in the last decades, there is a lack of knowledge of the global
58 seismic performance of systems that have been retrofitted [2].

59 A significant understanding has been accomplished on the flexural and shear strengthening, and on
60 confining individual structural elements, or bi-dimensional configurations of beam-column connections.
61 However, limited information is available on the highly complex 3-dimensional structural behavior [10].
62 Currently, there are few codes devoted to seismic strengthening of buildings. In consequence, engineering
63 discernment is commonly based on assessment methods that are conceptually appropriate to the design of
64 new structures, rather than assessing existing ones [11].

65 A literature review (2019) on retrofitting of RC buildings revealed different techniques developed in the
66 last decades and calibrated through experimental and numerical research [12,13]. Steel bracings, masonry
67 infills, and shear walls have shown the feasibility to increase the global strength and stiffness of elements
68 and structures. However, there are several drawbacks to this approach, which includes excessive increment
69 of stiffness. If this increment is not considered carefully using inelastic analysis and design process, it could
70 decrease the ductility of structures and then affect the global behavior of the building. The need for new
71 foundations or strengthening of the existing ones is usually a drawback. All these three techniques may
72 demand a large space to place bracings and walls, and this affects functionality in excess [14].

73 External jacketing of columns and beam-column joints with composites made of Fiber-Reinforced
74 Polymers (FRPs) has become a well-developed retrofitting technique for improving the seismic performance
75 of sub-standard RC buildings [15–18]. The improvement on the deformation and shear strength capacity of
76 jacketed members helps to prevent the fragile collapse mechanism of buildings with limited ductility.
77 Nevertheless, the axial strength capacity keeps roughly constant [19]. The axial load variation on columns is
78 an important subject to consider as the interaction between axial load and flexural-shear loads affects the
79 seismic performance of structures. Purposely, most of the available research studies have contemplated, for
80 easiness, a constant axial load. This simplification is a disadvantage of current assessment procedures of
81 real structures [10,20].

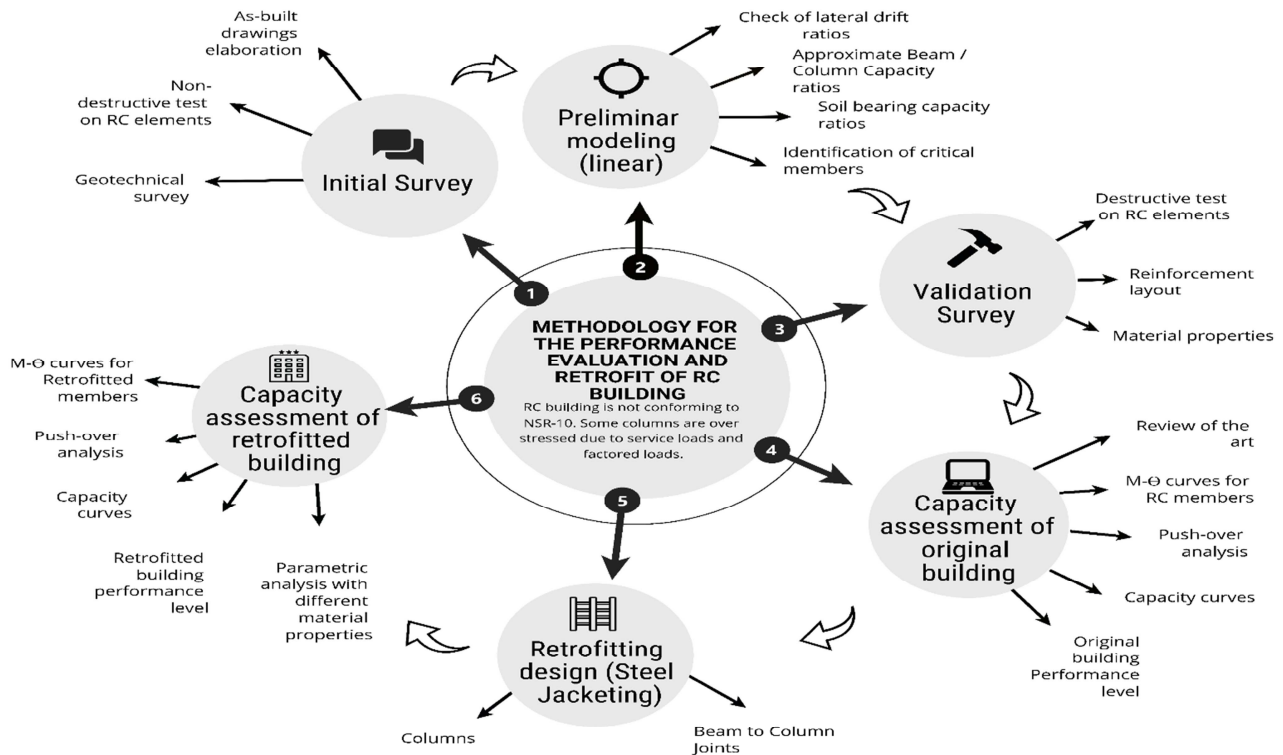
82 Another type of jacketing of columns and beam-column joints is based on steel elements. Different from
83 FRP jacketed RC buildings, steel jacketing of columns and beam-column joints could improve the shear
84 strength, the deformation capacity, and the global structural ductility and stiffness [21,22]. Besides, this
85 technique could overcome the challenge of space limitations related to other techniques like steel bracings,
86 masonry infills, or shear walls. The selection of an adequate retrofitting technique depends on desired
87 performance levels, economic criteria, and non-technical judgment [13]. In this study, a steel jacketing of
88 columns and beam-column joints is selected, considering the limitation of the building under study that is
89 related to overstressed columns under service loads, unavailability of space for bracings, or walls, and the
90 difficulty to build new foundations or to upgrade existing ones.

91 This paper shows the results of the seismic performance assessment and the retrofit design for a six-
92 story RC building in Cartagena de Indias (Colombia). It is part of a research project that aims at studying the
93 seismic performance of buildings not complying with service loads according to modern design codes. The
94 building was designed and constructed as a six-story non-conforming to NSR-10 [8] in 2010. In 2017,
95 another six-story building collapsed in the mentioned city for several non-compliances to Colombian seismic
96 code. In consequence, some owners contracted the study to assess the seismic performance of existing
97 buildings strictly considering elastic demand/capacity ratios and drifts, which is too limited.

98 This article deals with the effects of a selected steel jacketing retrofitting system on the original
 99 structure. The 3-dimensional building lateral strength, ductility, resistant base shear, the seismic response
 100 modification factor, R , and performance level [23,24] are studied using the capacity curves of both the
 101 existing building and the upgraded building. Besides, the increase of the columns compressive and flexural
 102 strength is set, using analytical expressions [25,26]. Finally, a parametric analysis of different concrete
 103 properties of the existing building, and load scenarios are provided.

104 2 MATERIALS AND METHODS

105 As a first step of the study (Fig. 1), initial surveys were performed to define the structural prototype. A
 106 geotechnical survey, non-destructive tests on RC elements, and As-built drawings elaboration were
 107 included. According to Vesic, Meyerhof, Terzaghi, and Hanzen's theories [27,28], ultimate pressure is 1000
 108 kPa; this soil bearing capacity is considerably high when compared to other soils of foundation in Cartagena.
 109 In the second step (Fig. 1), a preliminary linear-model of the existing building was made to check lateral drift
 110 ratios, beams/columns capacity ratios, and soil bearing capacity ratios. Thereby to identify the critical
 111 members.
 112
 113



114
 115 **Figure 1** Flowchart for assessment and retrofit of the RC model structure.

116 The structural prototype is a six-story residential building in Cartagena de Indias, Colombia. As shown
 117 in Figure 2, the architectural plan configuration is rectangular-shaped and irregular because axis 3 is not
 118 parallel to others, and axis 2 is not continuous all along the building length and the reduction of columns in
 119 frames along the "Y" direction. The plan of the building is 21.05 m long and 11.10 m wide. RC moment-
 120 resisting frames in both directions provide a seismic force resistance system. Considering that design and
 121 "As-built drawings" were not available, a structural survey was developed in step 3 (Fig. 1) to investigate the

122 reinforcement layout and to validate existing material properties. This step included a destructive test on RC
 123 elements (Fig. 3, Tables 1 and 2).
 124

125 **Table 1** Dimensions and reinforcement details of RC columns.

Column type	Dimensions (mm)	Reinforcement						
		Longitudinal			Transversal			
		Rebar	Area (mm ²)	Ratio (%)	Rebar	Area (mm ²)	Spacing (mm)	Confinement length (mm)
Typical	250 x 500	6 Ø 20 + 2 Ø 16	2100	1.68	2 Ø 9	138	100 / 200	500

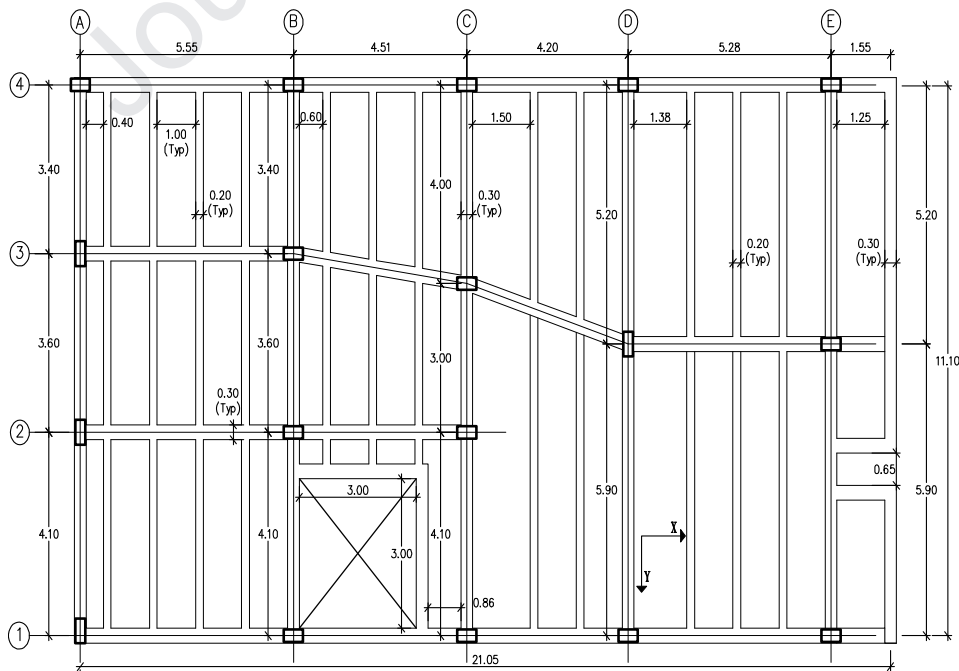
126

127 **Table 2** Dimensions and reinforcement details of RC beams.

Beam Type	Dimensions (mm)	Reinforcement					
		Longitudinal		Transversal			
		Top rebar (ratio, ρ)	Bottom rebar (ratio, ρ)	Rebar	Area (mm ²)	Spacing (mm)	Confinement length (mm)
Structural system (TYP.)	300 X 300	2 Ø 20 (0.0076)	2 Ø 20 (0.0076)	2 Ø 9	138	200	0
Joists	200 x 300	2 Ø 16 (0.0067)	2 Ø 16 (0.0067)	2 Ø 9	138	200	0

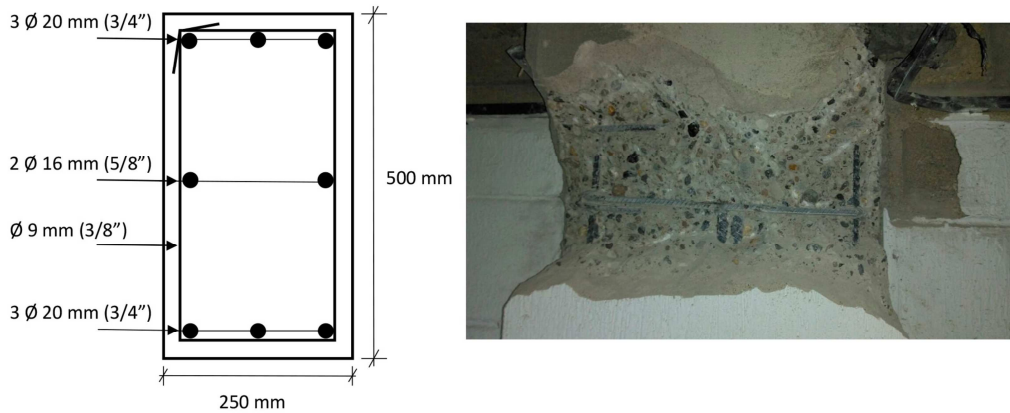
128

129 The hooks for beam/column stirrups are closed to 90°, not to 135°, as required by NSR-10 for seismic
 130 purposes. The columns' reinforcement is distributed symmetrically along the column sides.
 131



132

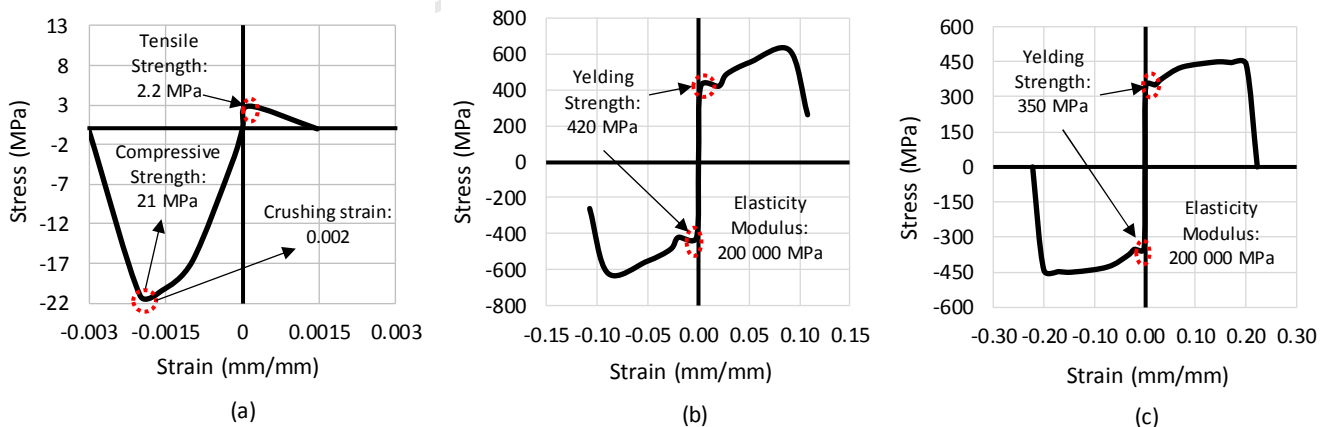
133

Figure 2 Typical floor plan of the prototype building.134
135**Figure 3** Scarification of structural elements to determine existing reinforcement.

136 The typical story height of the building is 2.80 m. The specified compressive strength of concrete (f'_c) is
 137 21 MPa and reinforcing steel bars comply with ASTM A615, Grade 60 steel ($f_y = 420$ MPa; $E = 200$ GPa).
 138 According to NSR-10 code, the live load for living rooms is 1.8 kPa, 3.0 kPa for stairs, and 5.0 kPa for
 139 balconies. The dead load is 4.6 kPa, which includes the weights of floor cover and the partition walls. Self-
 140 weight from other structural elements like the RC slab ($t = 120$ mm), columns, and beams are computed by
 141 the finite element analysis software (Section 3).

142 Figure 4 shows the stress-strain material models used for push-over modeling. Concrete follows a non-
 143 linear uniaxial constant confinement model [29–31]. Steel reinforcement (rebar) and steel angles for
 144 retrofitting (Section 4) were modeled with a simplified version of the Ramberg-Osgood model [30,31] cited
 145 by Elkholy & Ariss [32], using the software. The geotechnical survey displayed a high soil performance
 146 level, and therefore, the discussion of the performance of the building is centered on the structural non-
 147 compliances.

148



149

150

Figure 4 Material models. Stress-strain curve (a) for concrete, (b) for steel reinforcement bars, (c) for steel angles

151 Lateral loads were computed as per NSR-10 code, chapter A.10: Assessment, retrofitting, or
 152 rehabilitation [24,33]. The seismic mass is equal to the dead load. A “C” soil profile, characterized by dense
 153 soil or soft stone with a shear wave velocity varying between 360 and 760 m/s and STP number $N \geq 50$, was
 154 considered for evaluating the bearing capacity. Site seismic parameters and the building location resulted in

155 a design ground acceleration of 0.05 g, associated with a 20 % probability of exceedance in 50 years. This
 156 exceedance is permitted by NSR-10 only for assessment, upgrade, rehabilitation, or retrofitting of the
 157 structural system of pre-existing buildings. The assessment considered a response modification coefficient
 158 (R) of two (2). The load combinations followed the Colombian code, which are the same combinations as
 159 ASCE 7-10.

160 The fourth step of the investigation (Fig. 1) consisted of the capacity assessment of the existing
 161 building. A review of the seismic performance literature related to building retrofitting was made before the
 162 selection of the retrofitting technique. An analysis of $M - \phi$ curves for RC members and capacity curves
 163 were considered to determine the performance level of the original building. The retrofitting scheme was
 164 planned considering the strong column-weak beam principle. The steel jacketing details of RC columns and
 165 joints were determined in step five (Fig. 1) and are described in the following sections. Finally, the sixth step
 166 (Fig. 1) aimed at the capacity assessment of the retrofitted building. Capacity curves for the steel-jacketed
 167 RC building were obtained for the two main orthogonal directions. The effects of the selected steel jacketing
 168 scheme on the seismic performance of the building are discussed. Ductility, lateral strength, and the
 169 influence of different concrete properties of the existing structure are some parameters considered in the
 170 analysis.

171 3 THEORY/CALCULATION OF THE EXISTING BUILDING RESPONSE

172 The numerical model of the RC building was a 3D frame, rigidly connected at beam-column joints and
 173 diaphragms (Fig. 5). A Response Spectrum Analysis (RSA) and a Modal Push-over Analysis (MPA) were
 174 carried out using SAP2000v20 finite element method software [34]. Geometric and material non-linearities
 175 were considered to predict the behavior of the structure under static and dynamic loads.
 176



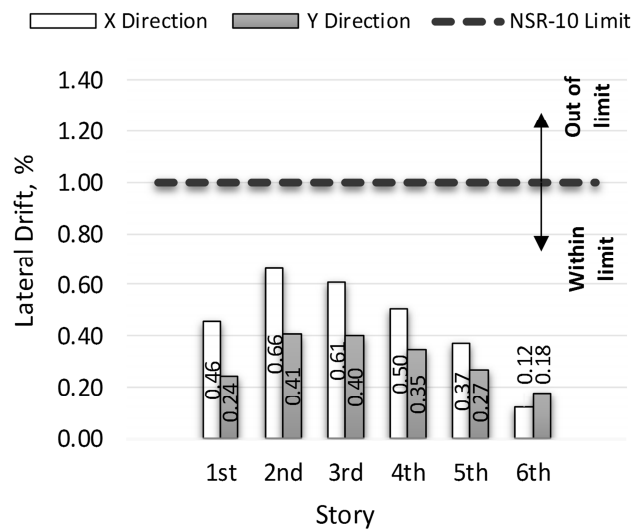
177
 178 **Figure 5** Left: Existing RC building. Right: Original building Model.

179 3.1 Modal Response Spectrum Analysis (MRSa)

180 The MRSa is a standardized method to evaluate structures performance subjected to lateral loads. The
 181 following relevant parameters help to understand the structural behavior and response mechanisms.

182 3.1.1 Lateral inter-story drift

183 Lateral inter-story drift is computed as a percentage (%) of story height. Figure 6 shows the maximum values for the drifts along the main orthogonal directions of the structure (named X and Y), for every story of the building. As shown in Figure 6, lateral story drifts meet the drift limit specified by NSR-10 (1 % of the total floor height). However, it shall be considered that seismic movements with a 20 % probability of exceedance in 50 years, for assessment of existing buildings, correspond to a limited-safety performance level, according to NSR-10 [8], equivalent to collapse-prevention in FEMA 440 [23]. For the design of new buildings, movements with a 10 % probability of exceedance in 50 years would be taken into account, and the lateral stiffness of the structure would need to be increased to reduce drift values in compliance with the maximum allowable drift.



192
193 **Figure 6** Maximum lateral story drift for the existing building associated with critical load combinations along the main
194 orthogonal directions (X and Y).

195 3.1.2 Required/provided normalized reinforcement area

196 The criteria for demand/capacity assessment took into account the required/provided normalized
197 reinforcement area in structural columns. Namely, the rebar area divided by the gross area of the column
198 sections. Figs. 7a, 7b, and 7c summarize the demand/capacity assessment. Three load scenarios have
199 been considered: vertical service loads, vertical factored loads, and seismic load combinations. As PROV
200 designates the normalized reinforcement area provided for the original columns. As LIM RC (NSR) refers to
201 the limit for the normalized area to avoid over reinforcing of RC columns, according to NSR-10 [8], set as 4
202 %.

203 It is noted in figure 7a that, for vertical service loads, there are two columns (D3 and E3) requiring more
204 than 200 % of provided normalized reinforcement area on the first floor (4.27/1.68 and 3.64/1.68,
205 respectively). These two same columns are demanding 5 % and 1 % more reinforcement than provided on
206 the second floor (1.76/1.68 and 1.69/1.68, respectively). This same observation is available in figures 7b and
207 7c for the other two load scenarios. For the most critical load combination (seismic load), nine (9) of 18
208 columns required retrofitting on the first floor, seven (7) on the second floor, two (2) on the third floor, and
209 one (1) at the fourth floor. Nineteen (19) of 54 columns require an upgrade for compressive or flexural
210 strength or both. Nevertheless, due to durability and constructional issues, 22 columns-joints need
211 retrofitting (subsection 3.3 shows the scheme proposed): 11 in the story one, 8 in story two, 2 in story three
212 and 1 in story four.

213

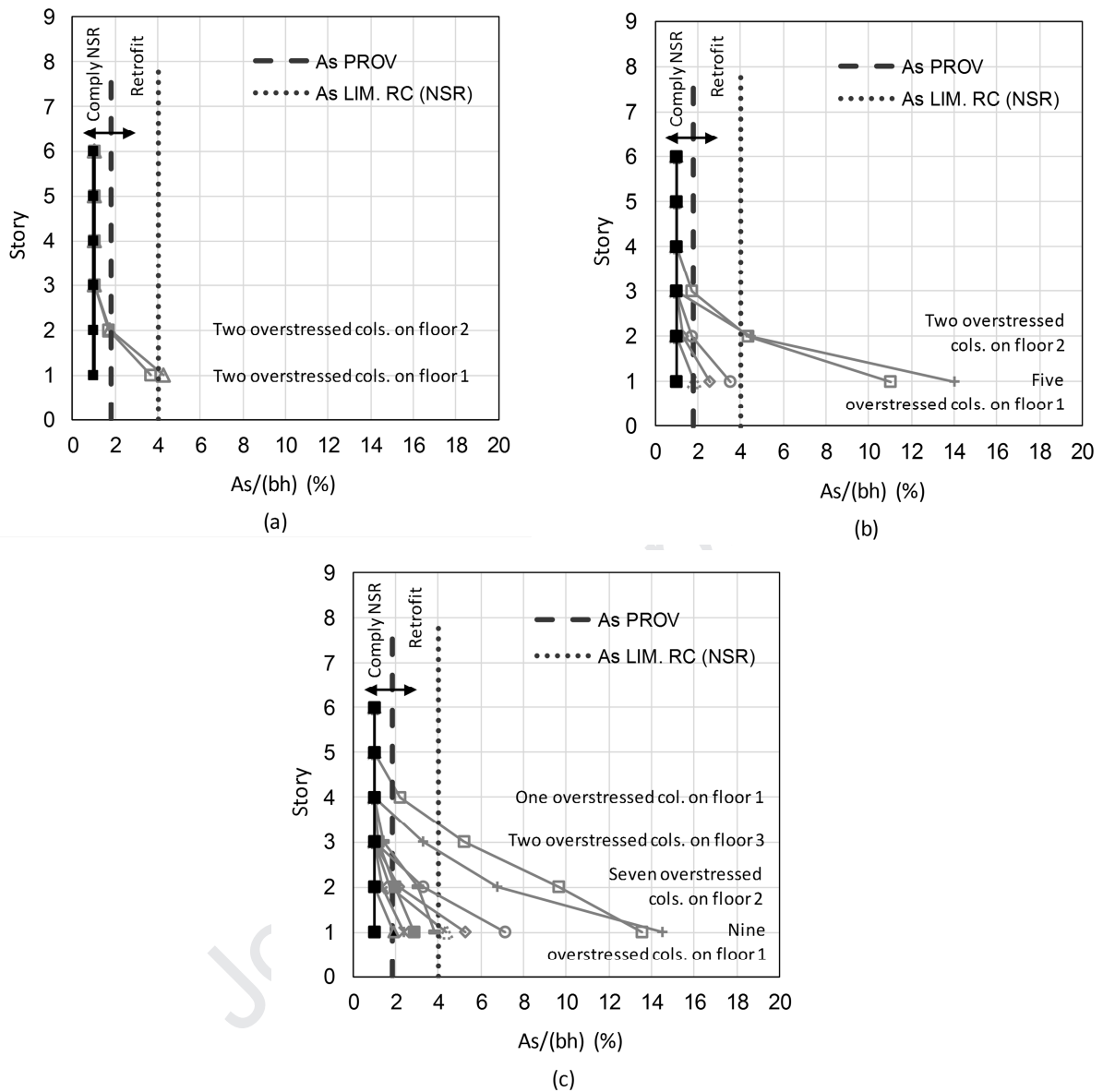


Figure 7 Provided vs. required reinforcement area in original columns for a) vertical service loads, b) factored vertical loads, c) seismic load combinations.

The considerations of demand/capacity for beams and footings are similar to those related to the columns. Beams and footings comply with the seismic code in terms of flexural strength limit. For typical beams, the critical required reinforcing area for bending is 400 mm^2 according to the software outputs, and the provided reinforcing area for bending is 567 mm^2 . The slab and beams of the original structure behave as composite members, but conservatively, the numerical model fails in considering this composite action. The same situation for required/provided reinforcement occurs for footings, which, the most critical footing requires $1387 \text{ mm}^2/\text{m}$, and the provided reinforcing area is $1425 \text{ mm}^2/\text{m}$ (1 # 6 @ 200 mm).

3.2 Modal Push-over Analysis (MPA)

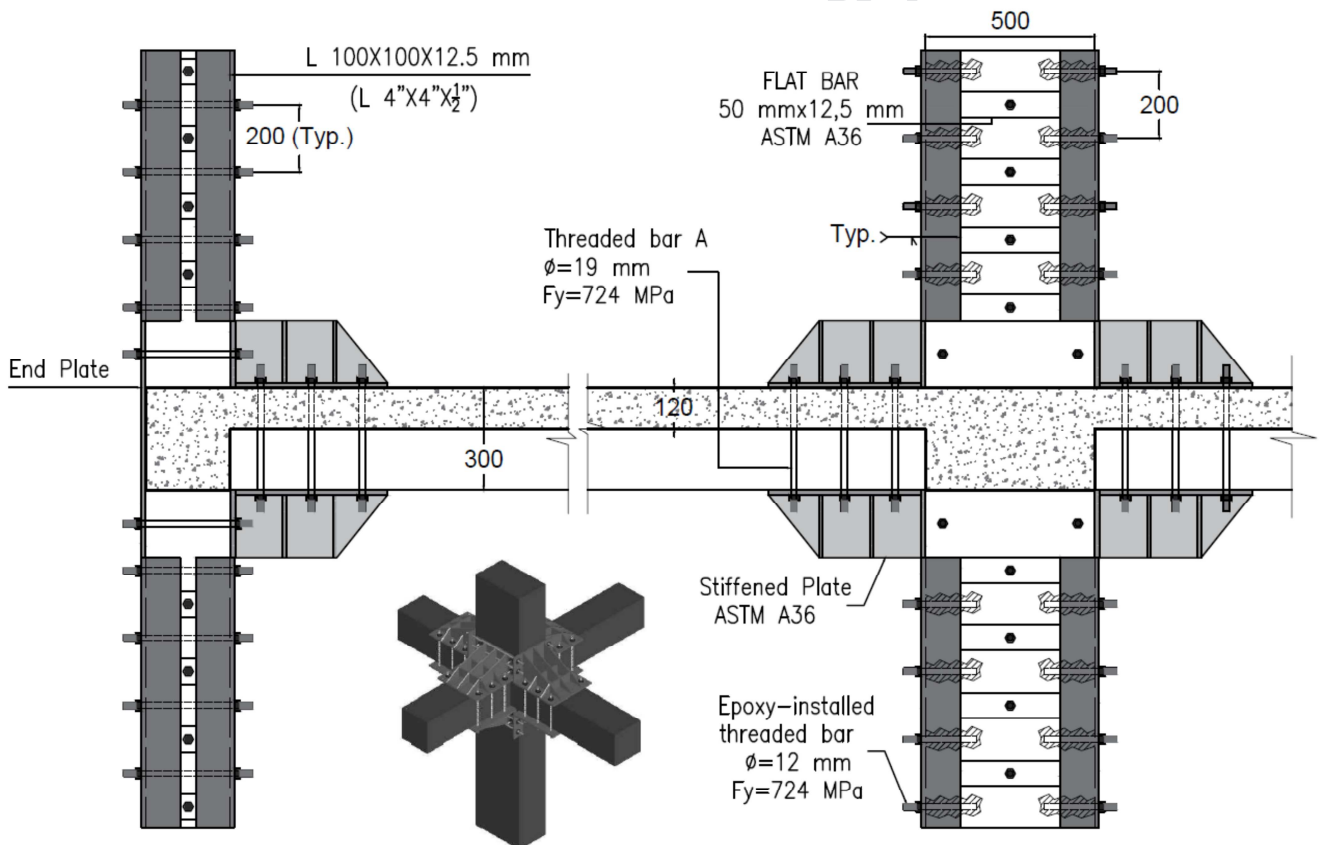
The seismic assessment of a building will require consideration of its non-linear response [35]. A major challenge in performance-based earthquake engineering is to develop simple and practical methods for estimating the capacity level and seismic demand on structures considering their inelastic behavior [36].

247 Incremental Dynamic Analysis (IDA) has recently arisen as a comprehensive non-linear analysis method.
 248 However, it is also recognized as computationally extremely demanding for practical cases [37–39].

249 The push-over analysis is one of the most widely used tools for seismic assessment of structures [40].
 250 An improved push-over method termed Modal Push-over Analysis (MPA) is selected in this study, which has
 251 shown a satisfactory degree of accuracy even in higher modes [23,38,41], and a trade-off between accuracy
 252 and simplicity. Subsection 4.2 shows the capacity curves for the existing and retrofitted building in the study.
 253 Section 5 presents the discussion of the stiffness, the ductility, and the seismic response modification factors
 254 based on the capacity curves.

255 3.3 Steel Jacketing Design

256 This study evaluates a steel jacketing retrofitting method to upgrade non-conforming buildings to current
 257 seismic codes. A literature review and numerical modeling performance conducted to the proposed steel
 258 jacketing details. The proposed retrofitting scheme involves steel angles covering 1/3 of column length
 259 above and below of each joint (for improving flexural capacity), covering the entire length of columns (for
 260 improving axial strength), and stiffened plates for RC beams. The connection between RC columns, beams,
 261 and retrofitting elements is performed through post-installed threaded bars spaced 200 mm (Fig. 8).
 262



263
 264

Figure 8 Retrofitting scheme for RC columns and beam-column joints.

265 3.3.1. Prediction of the compressive strength of columns

266 According to NSR-10 and ACI 318 [25], the axial strength design for a cross section (ϕP_{n1}) of existing
 267 columns is estimated using equation (1).
 268

$$\phi P_{n1} = 0.75\phi \left[0.85f'_c (A_g - A_{sr}) + f_{ysr} A_{sr} \right] \quad (1)$$

269 Where ϕ is the strength reduction factor, f'_c is the compressive strength of concrete, A_g is the gross
 270 area of the concrete section, A_{sr} is the total area of longitudinal reinforcement, and f_{ysr} is the rebar yield
 271 strength. Considering the material properties (Fig. 4) and dimensions of structural elements for the prototype
 272 building (Fig. 5 and Table 1), the analytical compressive strength of existing columns ϕP_{n1} is 1533 kN. The
 273 MRSA for the existing building helped to identify that the critical compressive load on existing columns is
 274 close to 2251 kN. Hence, the columns are overstressed. Given the overstress of existing columns due to
 275 vertical loads, one purpose of the retrofitting is to provide additional axial strength immediately to the
 276 columns, working as a composite member promptly. On the opposite, some retrofitting techniques, like FRP
 277 jacketing, work by confinement and require that columns deform axially so that the jacketing gets fully
 278 activated [19].

279 Compressive strength of retrofitted columns, ϕP_{n2} , is calculated using requirements prescribed by NSR-
 280 10 and by AISC 360 [26] specifications for composite members, equations (2) to (6).
 281

$$\text{For } P_e \geq 0.44P_{no} \Rightarrow \phi P_{n2} = \phi P_{no} \left[0.658^{(P_{no}/P_e)} \right] \quad (2)$$

282 Where P_e is the elastic critical buckling load, which is computed using equation (3).
 283

$$P_e = \pi^2 (EI_{eff}) / L_c^2 \quad (3)$$

284 EI_{eff} expresses the stiffness of the composite section, L_c is the effective length of the member (KL),
 285 K is the effective length factor, and L is the length of the member. EI_{eff} is estimated with equation (4).

$$EI_{eff} = E_s I_s + E_s I_{sr} + C_1 E_c I_c \quad (4)$$

286 E_s is the modulus of elasticity of steel (200 000 MPa), E_c is the modulus of elasticity of concrete (
 287 $0.043 \times w_c \times \sqrt{f'_c}$), and w_c is the weight of concrete per unit volume (24 kN/m³). I_s is the moment of inertia of
 288 the steel shape about the elastic neutral axis of the composite section, I_{sr} is the moment of inertia of the
 289 reinforcing bars about the elastic neutral axis of the composite section, and I_c is the moment of inertia of the
 290 concrete section about the elastic neutral axis of the composite section. C_1 is the coefficient for calculation
 291 of effective rigidity of an encased composite compression member, computed using equation (5).
 292

$$C_1 = 0.25 + 3 \left(\frac{A_s + A_{sr}}{A_g} \right) \leq 0.7 \quad (5)$$

293 The variable P_{no} , used in eq. (2), is computed according to equation (6).
 294

$$P_{no} = f_y A_s + f_{ysr} A_{sr} + 0.85f'_c A_c \quad (6)$$

295 Where f_{ysr} and f'_c were defined for eq. (1) and f_y is the minimum yield strength of the steel section.
 296 Accordingly, to the case under study (Fig. 5 and Table 1), the analytical compressive strength of retrofitted
 297 columns, ϕP_{n2} , is 4410 kN. Note that the computed compressive strength of retrofitted columns is 287 %

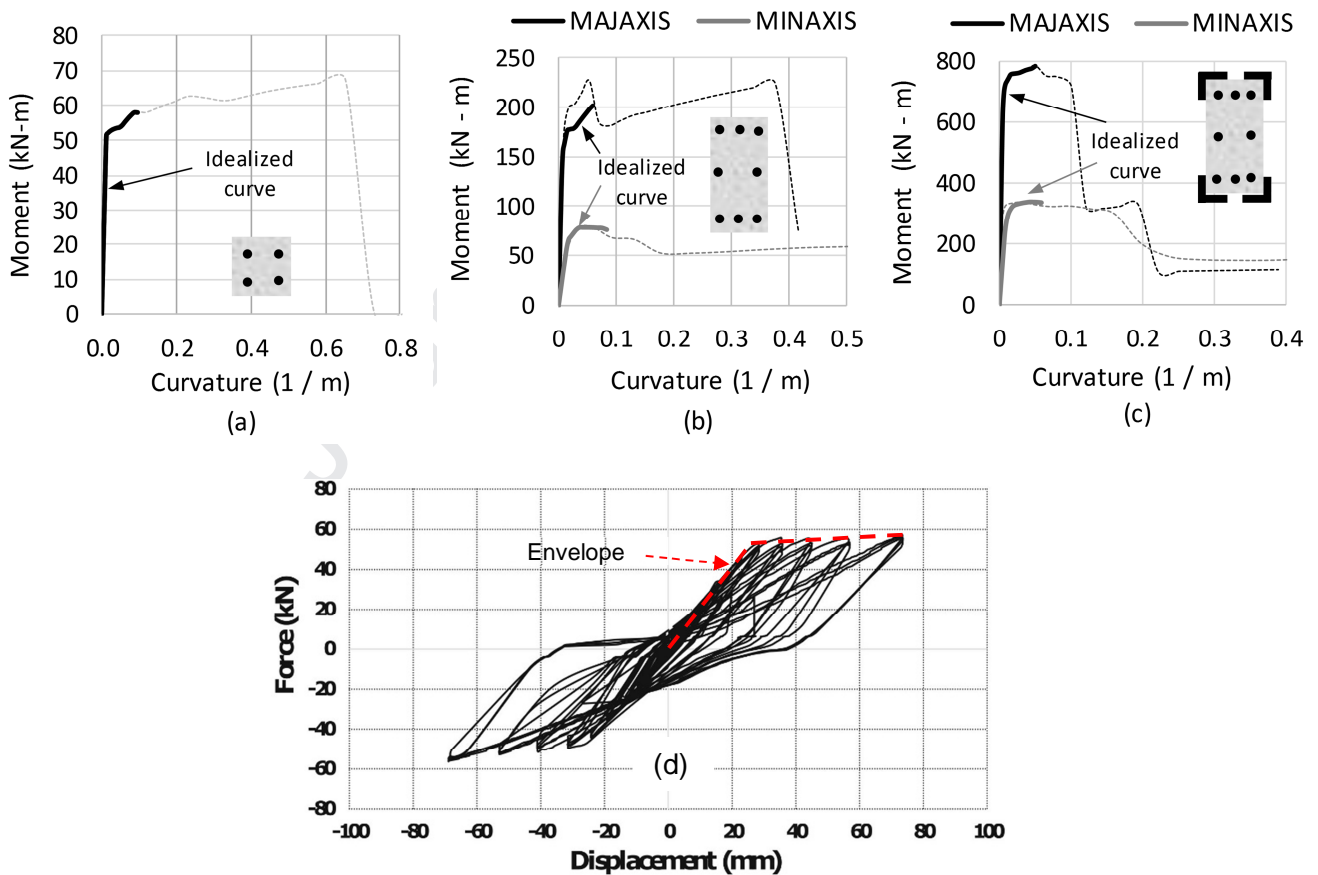
298 higher than that of existing columns. This compressive strength is enough to resist the elastic strength
 299 demand of load combinations prescribed by NSR-10. Further discussion is presented in section 5.

300 3.3.2. Beams, columns, and joints flexural properties

301 Section Designer, built into the software from CSI [34], facilitates the estimation of flexural properties of
 302 beams, columns, and joints. Section Designer is an integrated utility that enables the modeling and analysis
 303 of custom cross sections. This tool is useful to evaluate the flexural properties and non-linear responses of
 304 the members, including non-linear hinges. Figure 9 summarizes the flexural properties of the retrofit scheme
 305 and original members.

306 The actual modeled curves show a post-peak degradation. Notice that degradation is more prominent
 307 for retrofitted columns (Fig. 9c) than for original columns (Fig. 9b), for major and minor axis, designated as
 308 MAJAXIS and MINAXIS in figures 9b y 9c, respectively. This degradation is associated with the fact that
 309 retrofitting generates that failure strain in concrete is reached earlier than the yield strain of steel angles
 310 is reached. Besides, notice that a strain hardening effect is shown for original columns properties (Fig. 9b)
 311 after the yielding moment is reached.

312 In order to compensate for post-peak degradation, Idealized curves are considered, meeting ASCE 41-
 313 17 [24] to define non-linear hinges. The paper compares the numerical results for the beam to existing
 314 experimental data of a sub-assembly with a similar retrofitting scheme and beam specifications [22], in
 315 section 5.
 316

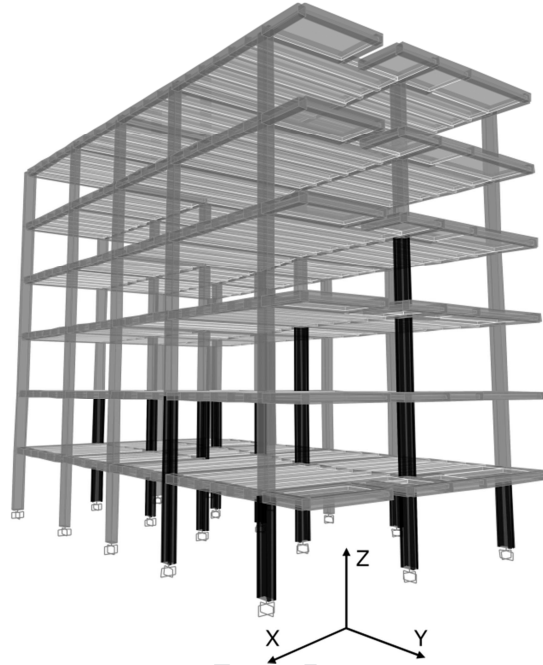


317
 318
 319
 320
 321
 322
 323
 324
 325
 326
 327
 328
 329
 330
 331

332 **Figure 9** M-Curvature diagrams of structural elements: (a) 300 mm x 300 mm existing RC beam, (b) 250 mm x 500 mm
 333 existing RC column, (c) 250 mm x 500 mm retrofitted RC column, (d) Hysteretic response of a previous study with
 334 similar retrofitted joint scheme [22]

335 4 RESULTS OF THE EVALUATION OF THE RETROFITTED BUILDING

336 Figure 10 shows the numerical model of the retrofitted building, which comprises a 3D frame with beam-
 337 column joints properties according to the proposed retrofit scheme (Fig. 8). A MRSA and a MPA were
 338 carried out using the software.

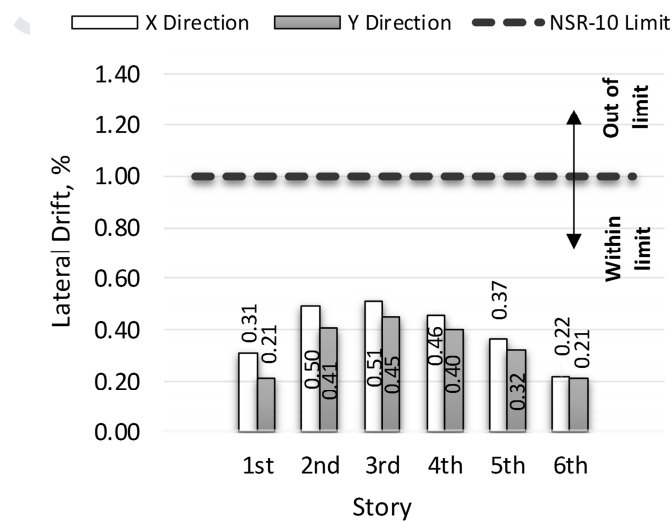


339
340 **Figure 10** Isometric view of the retrofitted building.

341 4.1. Modal Response Spectrum Analysis (MRSA)

342 4.1.1. Lateral inter-story drift

343 Lateral inter-story drifts for the retrofitted building are computed, similar to the existing building case.
 344 Figure 11 shows the results of the calculation. It can be noticed that the drift values are according to NSR-10
 345 requirements for all the stories. A discussion of the results is available in section 5.



346

347

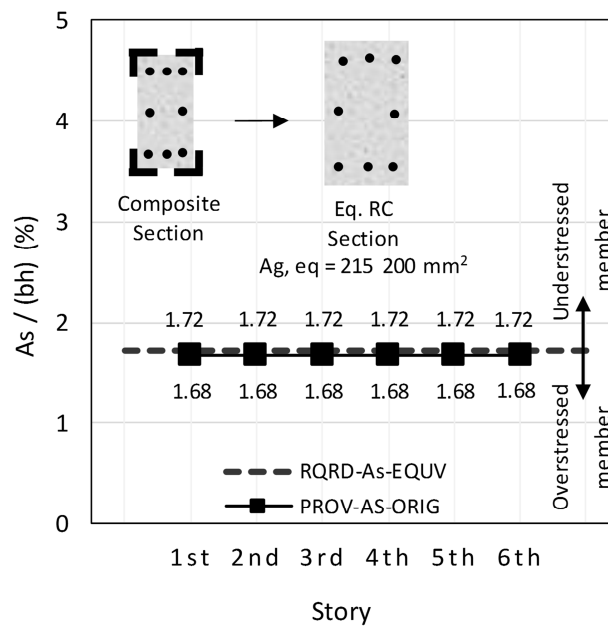
348

Figure 11 Maximum lateral inter-story drift for retrofitted building under critical load combinations along the main orthogonal directions (X and Y)

349

350 4.1.2. Required/provided reinforcing area

351 Figure 12 summarizes the results of required/provided normalized rebar area for columns, considering all
 352 the load combination cases. It is noticed in the figure that all columns require the minimum flexural
 353 reinforcing area, according to NSR-10 (1% of the cross-sectional area) on all floors. The Section Designer of
 354 the software considers an equivalent RC section for the retrofitted RC typical column (a composite section),
 355 with a cross section area equal to 215 200 mm². Thus, the minimum column normalized reinforcement is
 356 1.72 % (2512 mm²/1250 mm²). The provided normalized reinforcement area is 1.68 %, as stated in Table 1.
 357 The proposed retrofitting scheme practically eliminates the overstress on failing elements. RQRD-As-EQUV,
 358 in Figure 12, refers to the required rebar area for the equivalent RC section. PROV-As-ORIG refers to the
 359 provided reinforcing steel area for the original cross section of the column.
 360



361

362 **Figure 12** Provided vs. required reinforcing area in retrofitted columns for seismic load combinations.

363

364 4.2. Modal Push-over Analysis (MPA)

365 Figure 13 shows the deformed shape of the structure after the last step of the progressive lateral load
 366 applied to the retrofitted building along the “Y” direction. The colors of hinges represent the seismic
 367 performance levels according to AISC 360 [26], FEMA 440 [23], and ASCE 41 [24]. Although this loading
 368 step corresponds to near collapse or general instability, there are only a few orange or yellow hinges; in
 369 other words, a few hinges go far beyond collapse-prevention performance level.

370

Table 3 Building Seismic Performance according to FEMA 356

Building case	FEMA 356
Original Building	LS: Life-safety
Retrofitted Building	IO: Immediate-occupancy

371

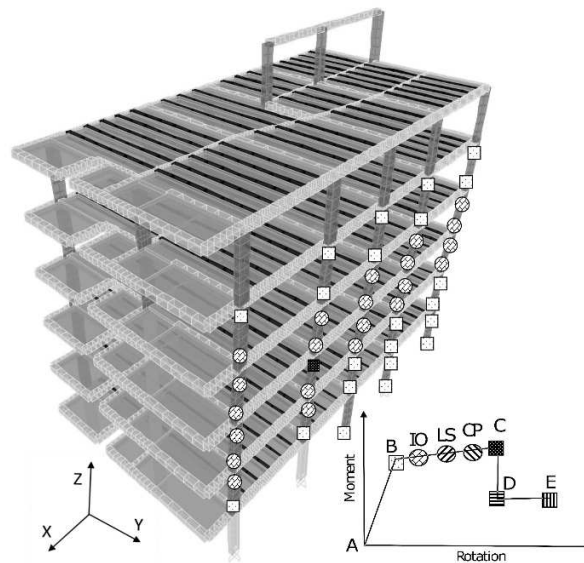


Figure 13 Building deformation after push-over lateral loads path along “Y” direction.

Figure 14 shows the capacity curve along “X” and “Y” directions for the original (designated as ORIGX and ORIGY, respectively) and for the retrofitted building (named RETRX and RETRY, respectively). The increased elastic strength of capacity curves reflects an improvement in the frame lateral strength. The target point (TP) defines the probable seismic performance of the building accordingly to site seismic movements evaluated.

The TP for the original building along “Y” direction corresponds to a seismic load slightly higher than the load related to the end of the linear behavior, which corresponds to the collapse-prevention level. Therefore, the original building shows good seismic performance along “Y” direction (Fig. 14).

On the opposite, Figure 14 shows that the TP for the retrofitted building along the “Y” direction corresponds to a seismic load slightly smaller than the one related to the end of linear behavior. The seismic performance of the retrofitted building along the “Y” direction corresponds to the immediate-occupancy performance level. Further analysis, considering other seismic load scenarios, and existing material properties are presented in Section 5.

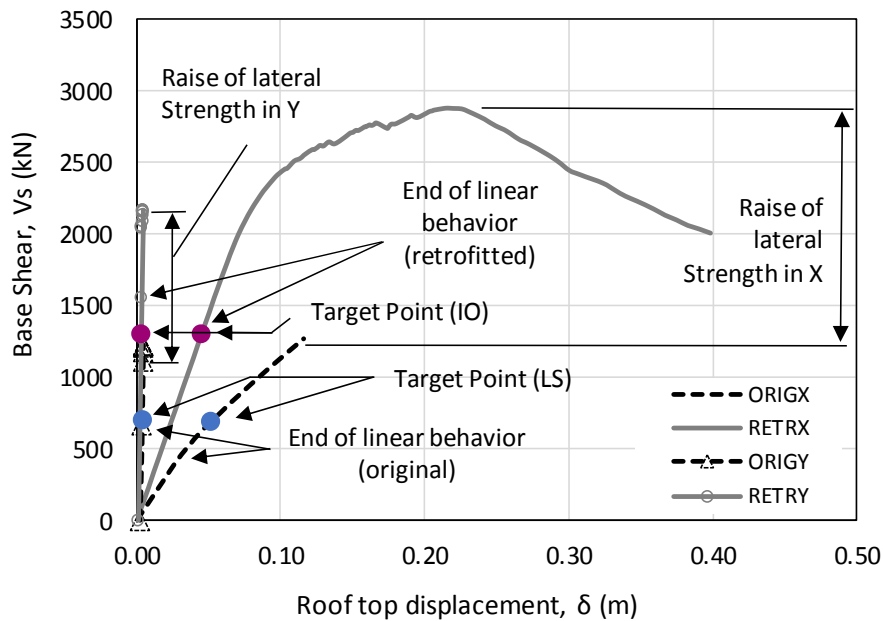


Figure 14 Capacity curve of the existing and retrofitted structure along X and Y directions.

Table 4 Target point data for retrofitted building according to FEMA 440

Description	Push-over X	Push-over Y
V_s [kN]	1305.45	1305.45
D [m]	0.045	0.00265
S_a [g]	0.077	0.077
S_d [m]	0.033	0.033
T_{eff} [s]	1.315	1.315
β_{eff} [%]	0.05	0.05
M	1	1

V_s : base shear. S_a : spectral acceleration. S_d : spectral displacement. β_{eff} : effective damping. T_{eff} : effective period. M : modification factor. D : rooftop displacement.

389
390
391

392 5 DISCUSSION OF RESULTS

393 Firstly, the structural safety of the building is improved by the steel jacketing design proposed. The
394 retrofitting allows the structure to comply with all the strength limit states of NSR-10 [8] seismic code. As
395 stated in the subsection, for service loads, there are two columns of the original building (D3 and E3, Fig. 2)
396 with required/provided rebar ratios equal to 2.53 and 2.16 on the first floor. This represents a high collapse
397 hazard.

398 Usually, demand/capacity ratios of 0.3 to 0.4 conform to all NSR-10 requirements. The
399 demand/capacity ratio of the retrofitted columns is 0.35 (1552kN / 4411kN), as determined in subsection
400 3.3.1., which is more reasonable for safety purposes. High axial demand/capacity ratios diminish the ductility
401 of columns and walls [42]. The increment of compressive column strength is 184 %.

402 The critical demand/capacity ratio due to axial loads on columns is an important criterion to select the
403 proposed retrofitting technique in this study. The selected steel jacketing (Fig. 8) can provide composite
404 action immediately after the retrofitting. Other techniques (e.g., FRP jacketing), which work by confinement
405 only, need that the original columns deform to activate the additional axial strength completely [19].

406 FEM analysis results exhibit a gain of column flexural capacity approximately equal to 261 % (Fig. 11),
 407 due to the steel jacketing. For instance, the retrofitted columns elastic-flexural-strength around the major
 408 axis is near to 552 kN-m (Fig. 11c), while the original columns elastic-flexural-strength is around 153 kN-m
 409 (Fig. 11b). Similar results are obtained around the minor axis of the column. The beams undergo a growth of
 410 51 % on the elastic-flexural-capacity. Figure 11a displays an original beam elastic-flexural-capacity of 53 kN-
 411 m, while Figure 11d corresponds to an elastic-flexural-capacity of about 81 kN-m (= 50 kN x 1.6 m).

412 The maximum story drift ratios for the original building are located on the second floor, along “X”
 413 direction (0.66 %) and along “Y” direction (0.41 %) (Fig. 6). It can also be noticed in Figure 6 that drifts get
 414 lower gradually from the second floor to the top, both for “X” and “Y” direction. The retrofitting reduces by 42
 415 % and 32 % the drift ratios in “X” direction on the first and second floor, respectively. This reduction at the
 416 lower floors is rational if it is considered that most of the retrofitted columns (and beam-column joints) are
 417 located on 1st (11 columns) and 2nd (8 columns) floors (subsection 4.1.1). The drifts for retrofitted building
 418 follows a similar pattern than for the original building (Fig.11). This substantial narrowing of story drifts
 419 represents a significant improvement on the seismic performance of non-structural-elements, given that
 420 structural displacements are recognized as a source of damage [9].

421 When comparing capacity curves in “X” and “Y” directions (Fig. 14), it can be observed that the global
 422 stiffness of the structure in the “Y” direction is higher than that in “X” direction, due to the redundancy along
 423 each direction. The elastic stiffness of the entire structure (K) can be defined as indicated in Table 5. The
 424 retrofitting increases the stiffness around 94 % in the “X” direction and practically does not increase the
 425 stiffness in the “Y” direction (1 % of the increment) (Table 5 summarizes the data for stiffness, extracted
 426 from Figure 14). This slight increment of stiffness along “Y” direction reflects that the seismic behavior along
 427 “Y” remains elastic for the retrofitted building, similar to the original building.

428 The resisting base shear of the building increase 127 % in “X” direction and 74 % in “Y” direction with
 429 proposed retrofitting (Fig. 14). Accordingly, the rooftop displacement for the retrofitted building is lower than
 430 for the original building, at target points.
 431

432

Table 5 Stiffness of retrofitted structure at linear behavior, K

Direction	Original Building K (kN/mm)	Retrofitted Building K (kN/mm)	Increment of K (%)
X	14.8 (= 433 kN / 29.1 mm)	28.8 (= 1551 kN / 53.9 mm)	94
Y	855.4 (= 1225 kN / 1.4 mm)	865.0 (= 1557 kN / 1.8 mm)	1

$K=V_{sy} / D$, where V_{sy} is the base shear at the end of linear behavior and D is the rooftop displacement at the end of linear behavior.

433

434

435

436

437

The global inelastic behavior of the retrofitted building suffers a substantial improvement. Ductility shows a rise of 40 % for “Y” direction, measured with strains at the ultimate resistant base shear. A similar analysis for the “X” direction of the building is performed, indicating an increment of ductility of 130 % in the building (Fig. 14 and Table 6).

438

Table 6 Analysis of ductility at the ultimate resistant base shear.

Direction	Original Building			Retrofitted Building			Increment of μ_{ult} %
	δ_{ult} (mm)	δ_y (mm)	μ_{ult}	δ_{ult} (mm)	δ_y (mm)	μ_{ult}	
X	113.7	31.2	3.65	398.2	47.4	8.40	130
Y	4.2	3.9	1.09	4.2	2.7	1.53	40

δ_{ult} : rooftop displacement at the ultimate resistant base shear. δ_y : displacement at the end of linear behavior. μ_{ult} : ductility at ultimate resistant base shear ($\mu_{ult}=\delta_{ult} / \delta_y$).

439

440

441

The MPA analysis path for the original building (Fig. 14) indicates that some elements use up their ultimate-flexural-strength before the target point load. For the “X” direction, 227 (of 1386) plastic hinges

442 exceed the immediate-occupancy (*IO*) performance level at the TP, although no hinges exceed the life-
 443 safety (*LS*) level. 226 (of 1386) plastic hinges exceed the *IO* performance level, and zero hinges exceed the
 444 *LS* performance level at the TP along the “Y” direction. The retrofitting reduces the number of plastic hinges
 445 exceeding the *IO* level. No hinges (of 1368) exceed *IO* performance level along “X” direction, and no hinges
 446 (of 1368) neither exceeds *IO* level in “Y” under TP loads.

447 It can be shown in figure 13 that a few columns hinge before connected beams, which is not appropriate
 448 [25]. This does not mean collapse. While some columns hinge, other columns and joints are still providing
 449 stiffness and strength to the building. Research involving an experimental test of a similar joint scheme [22],
 450 displays that retrofitting relocate the hinge on the beam further from the column face, as recommended by
 451 modern seismic standards to ensure a strong column-weak beam behavior [24].

452 One of the most valuable uses of non-linear analysis is to avoid the use of assumptions in the seismic
 453 response of the structure; for instance, the specified values of Seismic Response Modification factors (*R*)
 454 for the elastic method of structural analysis. *R*-values can be approximately calculated, extending a line
 455 from the elastic zone of capacity curves up to demand curves, for a specific design earthquake and
 456 structure, using MPA results (eq. 7).
 457

$$R = \frac{S_{a,pro}}{S_{a,d}} \quad (7)$$

458
 459 *R* : seismic response modification factor. $S_{a,pro}$: projected spectral acceleration, extending the elastic
 460 line of the capacity curve up to the demand curve (5 % reduced because of viscous damping). $S_{a,d}$: spectral
 461 displacement of the target point.
 462

463 Table 7 shows *R*-values according to MPA results.
 464

465 **Table 7** Seismic response modification factors, *R*, according to MPA results.

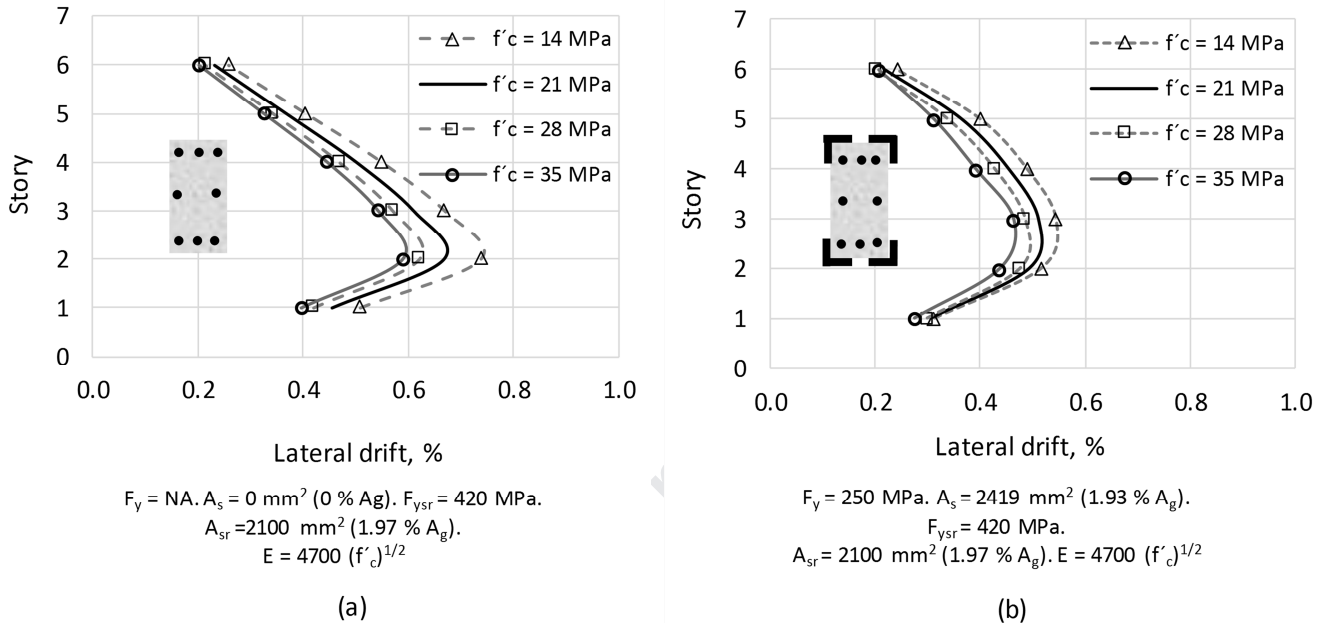
Description	Push-over X		Push-over Y	
	Original	Retrofitted	Original	Retrofitted
$S_{a,pro}$	0.069	0.08	0.069	0.079
S_d	0.04	0.033	0.04	0.033
<i>R</i>	1.73	2.42	1.68	2.39

466
 467 Despite figure 14 shows that the original building reaches a *LS* performance level, it has to be
 468 considered that seven columns are not in compliment with the NSR-10 strength-limit-states just for vertical
 469 loads (Fig.7b), which represents a limited structural safety. This reflects that, although the definition of the
 470 non-linear hinges, according to ASCE 41 [24], considers axial-flexural loads interaction, the MPA capacity
 471 curve (Fig.14) does not display the infringement of axial strength limit states in the assessment of the
 472 performance level.

473 The values of seismic response modification factors, *R*, computed from the MPA curves (Table 7) show
 474 an agreement with previously selected *R*-value for MRSA, equal to two (section 2). This means that the
 475 original building has a relatively low inelastic capacity, especially in “Y” direction, where the building resists
 476 seismic movements lineally.

477 The concrete core test is the most recommended method to assess the actual compressive strength of
 478 existing RC buildings, according to some standards like ACI [25] and NSR-10 [43]. However, it is usually a
 479 controversial parameter for evaluation given that results are affected by many factors (e.g., length-diameter
 480 ratio, moisture condition, and drilling process, among others), which can easily conduct to misinterpretation
 481 [44]. A parametric analysis with different concrete columns compressive strength has been made to evaluate
 482 the influence of concrete strength on the seismic drifts, and the compressive/flexural strength.

483 Figure 15a shows the lateral drifts of the original building with columns considering concrete strengths of
 484 14, 21, 28, and 35 MPa. The graphics indicate that the highest strength (35 MPa), does not provide
 485 significant changes in the drifts ratios, in comparison to the lowest strength (14 MPa), especially in the
 486 highest stories. For floors 4, 5, and 6, the change in lateral drift values is short (from 0.41 % to 0.33 % on
 487 floor 5). There is a 25 % change in the drifts ratios for stories 1, 2, and 3 (from 0.74 % for 35 MPa to 0.59 %
 488 for 14 MPa, at floor 2).



$$F_y = NA. A_s = 0 \text{ mm}^2 (0 \% A_g). F_{ysr} = 420 \text{ MPa.}$$

$$A_{sr} = 2100 \text{ mm}^2 (1.97 \% A_g).$$

$$E = 4700 (f'_c)^{1/2}$$

$$F_y = 250 \text{ MPa. } A_s = 2419 \text{ mm}^2 (1.93 \% A_g).$$

$$F_{ysr} = 420 \text{ MPa.}$$

$$A_{sr} = 2100 \text{ mm}^2 (1.97 \% A_g). E = 4700 (f'_c)^{1/2}$$

489 **Figure 15** Story drifts for different concrete compressive strength (a) Original building (b) Retrofitted building

490 Figure 15b shows the lateral drift ratios of the retrofitted building varying the concrete strength of
 491 columns from 14 to 35 MPa every 7 MPa. It can be observed that the influence of concrete compressive
 492 strength on the lateral drift ratios of the retrofitted building is even lower than that for the original building.
 493 The maximum change in the drifts values is represented in story 2, equal to 18 % (from 0.44 % for 35 MPa
 494 to 0.52 % for 14 MPa). Drifts at Floors 1 and 6 practically do not suffer changes. The pattern displayed
 495 exhibits that retrofitting reduces lateral drifts at floors 1 and 2, where the number of retrofitted columns is 19
 496 (of 22 in total).

497 Figure 16 shows the flexural and compressive capacity of retrofitted, designated as RETRFLEX and
 498 RETRCOMP, respectively, and the flexural and compressive strength of original columns, named
 499 ORIGFLEX and ORIGCOMP respectively, for different column concrete compressive strength. Results
 500 demonstrate that the strength does not have any influence on the flexural capacity of original nor retrofitted
 501 columns. Notice that the lowest two lines on the graphic are horizontal.

502 The compressive capacity of individual columns can be increased with a gain of the concrete column
 503 axial strength for both, original RC columns by 46 % (2245 kN for 35 MPa versus 1533 for 21 MPa) and
 504 Steel jacketing retrofitted columns by 26 % (5562 kN for 35 MPa versus 4411 for 21 MPa). Figure 16 shows
 505 that even for $f'_c = 14$ MPa (a low strength concrete), the proposed retrofitting could rise the axial capacity
 506 by 225 % (3823 kN versus 1177 kN) and then, upgrade the structure to reach the specified structural safety
 507 by ACI [25] and NSR-10 [43].
 508
 509
 510

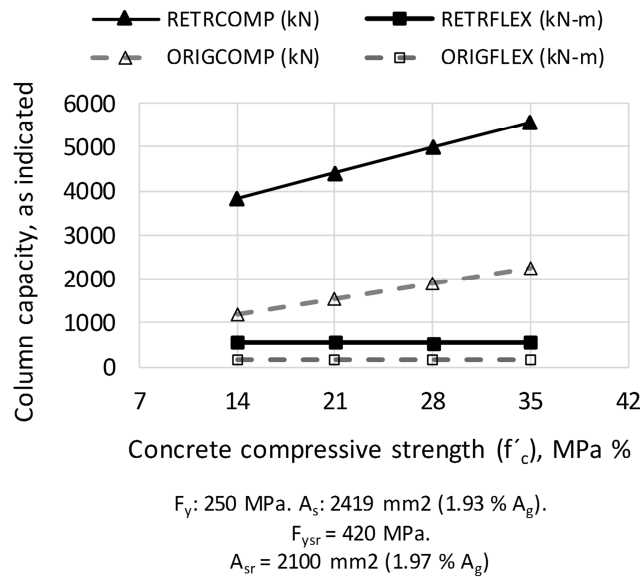


Figure 16 Columns capacity for different concrete compressive strength

511
512
513
514
515 The capacity curve for the retrofitted building in “X” direction (Fig. 14) displays a degradation post-peak
516 with a subsequent softening. This can be explained by the significant gain of ductility and lateral resistance
517 and by the absence of irregularities along the “X” direction. As the compressive strength of column-joint
518 does not influence on the flexural capacity (Fig. 16), the material models of the steel angles and rebars (Fig.
519 4) govern the path of the retrofitted curve in “X” direction. Probably, the columns rebar yields at about 2000
520 kN of base shear, causing an initial stiffness degradation, thus going far beyond their elastic limit until the
521 peak of the base shear, near to 2800 kN. Then, the steel angles get into plastic deformations, and the
522 retrofitted building shows another stiffness degradation (Fig. 14).

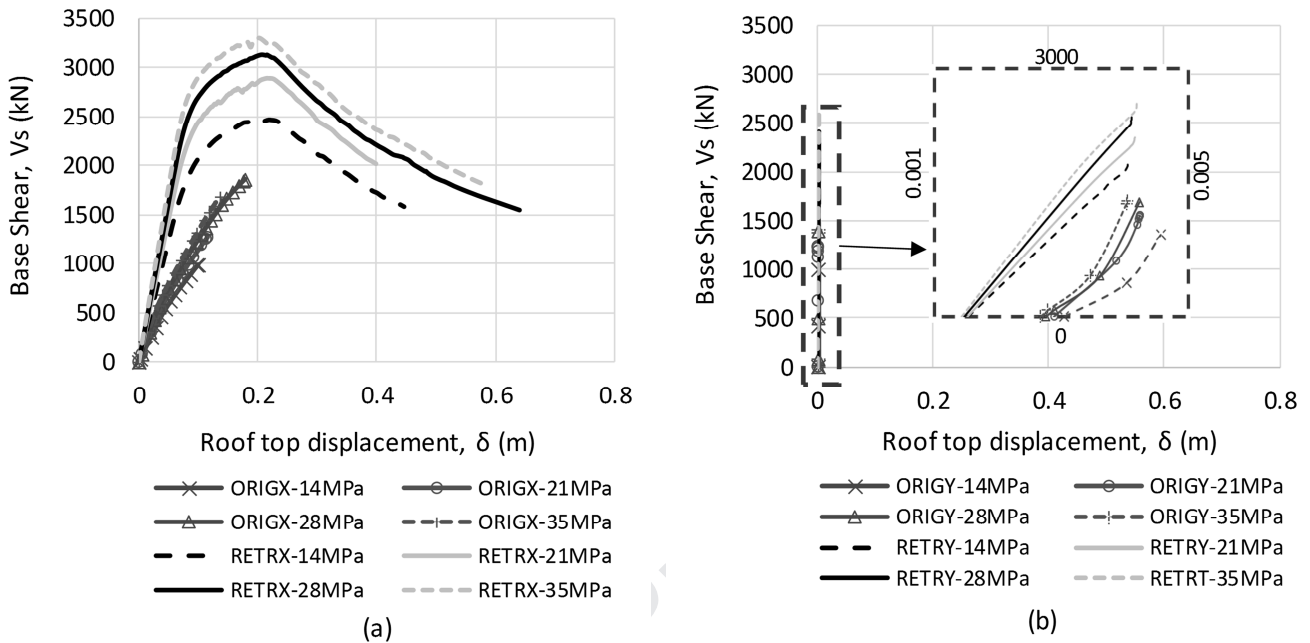
523 The original building in the “X” direction shows a shorter inelastic ability than the retrofitted building in
524 the same direction “X” (Fig. 14). Inelastic strains of rebars start at a base shear near to 500 kN, causing the
525 stiffness degradation up to the peak of the resisting base shear of about 1300 kN. However, in general,
526 capacity curves in direction “X” show better inelastic capacity than curves in “Y” direction (Fig. 14). The
527 reasons are that there are fewer columns in frames along “Y” direction than in frames along “X” direction, 14
528 of 18 columns are oriented with their minor axis in “Y” direction (Fig. 4) and the irregularity caused by the
529 reduction on the number of columns in axis D and E (Fig. 4). As redundancy of frames depends on the
530 number of columns, and ductility depends on redundancy, reasonably, the capacity curves in “Y” direction,
531 shows a non-ductile behavior for original and retrofitted building (elastic behavior).

532 The influence of the compressive strength of existing RC building on the capacity curves has been
533 estimated through a parametric analysis (Figs. 17a, and 17b) varying f'_c from 14 MPa to 35 MPa. The
534 capacity curves of the original building are designated as ORIGX-14MPa to ORIGX-35MPa for the “X”
535 direction and are designated as ORIGY-14MPa to ORIGY-35MPa for the “Y” direction. The maximum peaks
536 of the capacity curves in the “X” direction are proportional to the compressive strength of RC elements,
537 excepting for ORIGX-28MPa (Fig. 17a). Given that the axial strength does not affect the flexural capacity of
538 elements, the gain of resisting base shear of the building is due to the P-M interaction and the increment on
539 the Young Modulus of concrete. Then, for original columns, the limit to the raise on the base shear occurs
540 for 28 MPa. It is probable that for higher values of f'_c , the mechanism starts to be influenced more by
541 bending than by compression.

542 The capacity curves of the retrofitted building are designated as RETRX-14MPa to RETRX-35MPa for
543 the “X” direction and are designated as RETRY-14MPa to RETRY-35MPa for the “Y” direction. The
544 maximum peak of the capacity curves for the retrofitted building in the “X” direction, rounds 2881 kN for
545 RETRX-21MPa, and 3243 kN (Fig.17a) for RETRX-35MPa. This represents an increment of 13 %. In the

546
547
548

case of the original building, an increment of 30 % is given by a change in the resisting base shear from 1297 kN, to 1688 kN, for 21 MPa and 35 MPa, respectively.



549
550
551

Figure 17 Capacity curves for different concrete compressive strength a) “X” direction, b) “Y” direction

552 The capacity curves RETRX-14MPa to RETRX-35MPa (Fig. 17a) reflect that the ultimate rooftop
553 displacement not only depends on the compressive strength of concrete because there is not a constant
554 trend. The ultimate rooftop displacement for the retrofitted building depends on the interaction between the
555 compressive resistance of concrete and the strength of the steel of the retrofitting scheme (Fig. 8). However,
556 it shall be noticed that the degradation post-peak follows the same course for RETRX-14MPa to RETRX-
557 35MPa.

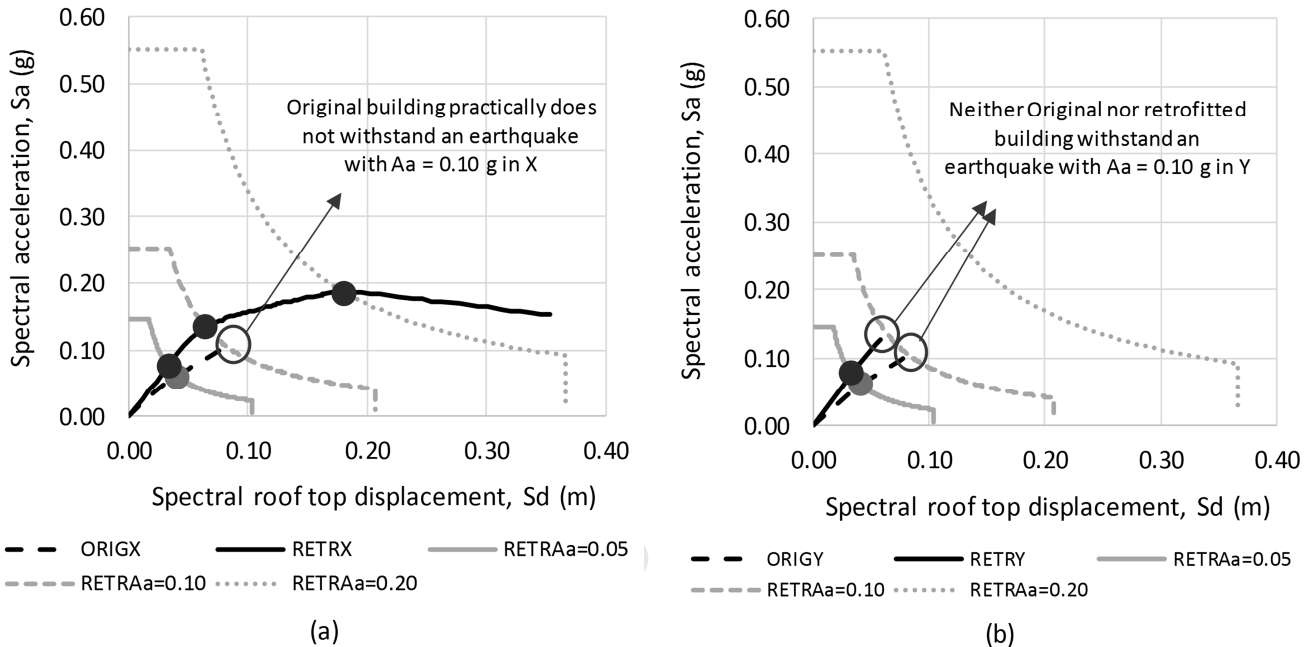
558 The influence of different compressive strength of concrete on the Ultimate rooftop displacements,
559 elastic stiffness, and maximum resisting base shear is not perceptible if the same axis scale as for the “X”
560 direction is used. Capacity curves need to be zoomed to notice any change (Fig. 17b).

561 Different values of concrete compressive strength practically do not affect the capacity curves along the
562 “Y” direction (Fig. 17b). The inelastic behavior in the “Y” direction is not considerable. Rebars and steel
563 angles do not yield when the failure mechanism appears. The failure is controlled by the geometry. There is
564 a less number of columns for frames along “Y” direction compared with the number for frames along “X”
565 direction, 78 % (14 of 18) of the columns are oriented with their minor axis in “Y” direction (Fig. 4) and the
566 irregularity of axis D and E (Fig. 4).

567 The capacity curves in the “Y” direction, shows a non-ductile behavior for all the cases, ORIGY-14MPa
568 to ORIGY-35MPa and RETRY-14MPa to RETRY-35MPa. Although the curve for the original building shows
569 an ascendant tendency, its structural behavior remains elastic (Fig. 17b). The capacity curves for retrofitted
570 building in “Y” direction (Fig. 17b) show an increment of 22 % in the maximum peak, represented by 2131
571 kN for RETRY-21MPa, and 2530 kN for RETRY-35MPa (Fig. 17b). Besides, the rooftop displacements for
572 the retrofitted building are similar for different concrete strengths. For the original building, displacements
573 increase 5 %, inversely to concrete strengths.

574 The influence of different seismic load scenarios on the capacity curves is analyzed. Seismic
575 movements with ground acceleration A_a of 0.10 g are designated as RETRAa=0.10. Movements with A_a of

576 0.20 g are designated as RETRAa=0.20, and seismic loads with A_a of 0.05 g are called RETRAa=0.05 (Figs.
 577 18a and 18b).
 578
 579



580
 581 **Figure 18** Capacity spectra for different seismic movements: a) "X" direction, b) "Y" direction
 582

583 RETRX in figure 18a shows that the retrofitted building can perform at LS level for all the load scenarios
 584 considered, along the "X" direction. On the opposite, although the demand spectra are reduced taking
 585 into account the effective period and damping of the structure as per FEMA 440 [23], it shall be noticed that
 586 in practical terms, the original building, designated as ORIGX is not able to sustain the seismic movements
 587 with A_a of 0.10 g nor 0.20 g (Fig. 18a). RETRY and ORIGY displays that the elastic behavior of both,
 588 retrofitted and original building, limit the ability to withstand earthquakes with A_a of 0.10 g and 0.20 g (Fig.
 589 18b).

590 A_a equal to 0.05 and 0.10 g corresponds to a low-seismic-hazard zone, and A_a of 0.20 corresponds to a
 591 moderate-seismic-hazard zone, according to NSR-10 [43]. Given the previous discussion, it can be stated
 592 that retrofitting allows the building to perform adequately for seismic movements of moderate-seismic-
 593 hazard zones in the "X" direction. Nonetheless, the geometry irregularities limit the safe performance along
 594 the "Y" direction, at low-seismic-hazard zones.

595 6 CONCLUSIONS

596 The results of this study demonstrated that the proposed retrofitting scheme enhances the individual
 597 axial and flexural column strength by 184 % and 261 %, respectively, and that the flexural resistance of
 598 individual columns is not influenced by the concrete compressive strength.

599 The steel jacketing raises the lateral strength of the building due to the stiffening of the joint of frames,
 600 by 127 % along the "X" direction and 74 % along the "Y" direction. An increment in the concrete strength
 601 from 21 MPa to 35 MPa, lead to an increment of 20 % in the lateral strength of the retrofitted and the original
 602 building; however, the influence in the seismic drifts is not so representative, as the highest reduction in the
 603 story drift values is of 0.1 %.

604 The non-linear behavior of the retrofitted building suffers an important improvement in comparison with
 605 the original building. Ductility increased 40 % for the “Y” direction and 130 % for the “X” direction. Concrete
 606 compressive strength has no substantial influence on ductility, nor the failure mechanism.

607 The geometrical irregularities along the “Y” direction of the prototype building limit the seismic
 608 performance of the structure at low-seismic-hazard zones. The retrofiting allows the global structure to
 609 ascend from life-safety to immediate-occupancy performance.

610 Acknowledgments

611 Authors thank the work of two students, Álvaro Hernández, and Roberto Babilonia, during their
 612 graduate thesis under the direction of the corresponding author. The help of Sebastian Pacheco during the
 613 revision process, as a research assistant, is especially valued. Besides, the comments from Oscar
 614 Coronado are appreciated, which have enhanced the quality of the figures, and the paper in general.

615 This research did not receive any specific grant from funding agencies in the public, commercial, or not-
 616 for-profit sectors. The third author acknowledges to Universidad Militar Nueva Granada in Bogotá, Colombia,
 617 for financing his research activities.

618 Declarations of interest: The authors declare that they have no known competing for financial interests
 619 or personal relationships that could have appeared to influence the work reported in this paper.

620 References

- 621 [1] H. Abou-Elfath, M. Ramadan, F. Omar Alkanai, Upgrading the seismic capacity of existing RC build-
 622 ings using buckling restrained braces, *Alexandria Engineering Journal*. 56 (2017) 251–262.
 623 <https://doi.org/10.1016/j.aej.2016.11.018>.
- 624 [2] J.P. Moehle, State of research on seismic retrofit of concrete building structures in the US, US-Japan
 625 Symposium and Workshop on Seismic Retrofit of Concrete Structures. (2000) 16.
- 626 [3] P. Ricci, F. De Luca, G.M. Verderame, 6th April 2009 L'Aquila earthquake, Italy: reinforced concrete
 627 building performance, *Bulletin of Earthquake Engineering*. 9 (2011) 285–305.
 628 <https://doi.org/10.1007/s10518-010-9204-8>.
- 629 [4] H. Sezen, A.S. Whittaker, K.J. Elwood, K.M. Mosalam, Performance of reinforced concrete buildings
 630 during the August 17, 1999 Kocaeli, Turkey earthquake, and seismic design and construction practise
 631 in Turkey, *Engineering Structures*. 25 (2003) 103–114. [https://doi.org/10.1016/S0141-0296\(02\)00121-9](https://doi.org/10.1016/S0141-0296(02)00121-9).
- 632 [5] V. Singh Rawat, Increasing the strength of existing building using steel jacketing in seismic zone, 2017.
 633 <https://doi.org/10.14445/23488352/IJCE-V4I12P102>.
- 634 [6] R.S. Aboutaha, M. Engelhardt, J.O. Jirsa, M.E. Kreger, Rehabilitation of shear critical concrete col-
 635 umns by use of rectangular steel jackets, 1999.
- 636 [7] H. Fukuyama, S. Sugano, Japanese seismic rehabilitation of concrete buildings after the Hyogoken-
 637 Nanbu Earthquake, *Cement and Concrete Composites*. 22 (2000) 59–79.
 638 [https://doi.org/10.1016/S0958-9465\(99\)00042-6](https://doi.org/10.1016/S0958-9465(99)00042-6).
- 639 [8] AIS, Reglamento colombiano de construcción sismo resistente, NSR-10, Asociación de ingeniería
 640 sísmica, Bogotá, Colombia, 2010.
- 641 [9] FEMA, FEMA 74. Reducing the Risks of Nonstructural Earthquake Damage. A Practical Guide, (1994).
 642 https://www.fema.gov/media-library-data/20130726-1721-25045-8384/fema_74_3rd_ed.pdf.
- 643 [10] S. Pampanin, U. Akguzel, G. Attanasi, Seismic Upgrading of 3-D Exterior R.C. Beam Column Joints
 644 Subjected To Bi-Directional Cyclic Loading Using GFRP Composites, 2019.
- 645 [11] J.M. Castro, M. Araújo, M. D’Aniello, R. Landolfo, Strengthening of RC Buildings with Steel Elements,
 646 in: A. Costa, A. Arêde, H. Varum (Eds.), *Strengthening and Retrofitting of Existing Structures*, Springer
 647 Singapore, Singapore, 2018: pp. 139–162. https://doi.org/10.1007/978-981-10-5858-5_6.
- 648 [12] J. Melo, D.A. Pohoryles, T. Rossetto, H. Varum, Performance comparison of RC retrofitted interior
 649 beam-column joints with CFRP and steel plates, 2017.
- 650 [13] Tsionis, Georgios, Taucer, Fabio, Apostolska, Roberta., Effectiveness of Techniques for Seismic
 651 Strengthening of RC Frame Buildings, in: 2015: pp. 1–8.
- 652

- 653 [14] F. Nateghi-A, Seismic strengthening of eightstorey RC apartment building using steel braces, *Engineering Structures*. 17 (1995) 455–461. [https://doi.org/10.1016/0141-0296\(95\)00071-E](https://doi.org/10.1016/0141-0296(95)00071-E).
- 654
- 655 [15] R. Azarm, M.R. Maheri, A. Torabi, Retrofitting RC Joints Using Flange-Bonded FRP Sheets, *Iranian*
656 *Journal of Science and Technology, Transactions of Civil Engineering*. 41 (2017) 27–35.
657 <https://doi.org/10.1007/s40996-016-0028-x>.
- 658 [16] A. Costa, A. Arêde, H. Varum, *Strengthening and Retrofitting of Existing Structures*, Springer Singa-
659 pore, 2017. <https://books.google.com.co/books?id=Ge85DwAAQBAJ>.
- 660 [17] S.A. Hadigheh, M. Maheri, S. Mahini, Performance of weak-beam, strong-column RC frames strength-
661 ened at the joints by FRP, 2013.
- 662 [18] C.Y. Osman Kaya Azadeh Parvin, and Selçuk Altay, Retrofitting of Reinforced Concrete Beam-Column
663 Joints by Composites—Part I: Experimental Study, *Structural Journal*. 116 (2019).
664 <https://doi.org/10.14359/51706922>.
- 665 [19] A. Ilki, E. Tore, C. Demir, M. Comert, Seismic Performance of a Full-Scale FRP Retrofitted Sub-
666 standard RC Building, in: K. Pitilakis (Ed.), *Recent Advances in Earthquake Engineering in Europe:*
667 *16th European Conference on Earthquake Engineering-Thessaloniki 2018*, Springer International Pub-
668 lishing, Cham, 2018: pp. 519–544. https://doi.org/10.1007/978-3-319-75741-4_22.
- 669 [20] U. Akguzel, S. Pampanin, Effect of Axial Load Variation on the Retrofit of Exterior Reinforced Concrete
670 Beam-Column Joints, 2019.
- 671 [21] N. Islam, M.M. Hoque, Strengthening of Reinforced Concrete Columns by Steel Jacketing: A State of
672 Review, *Asian Transactions on Engineering (ATE)*. 05 (2015).
- 673 [22] A. Torabi, M.R. Maheri, Seismic Repair and Retrofit of RC Beam-Column Joints Using Stiffened Steel
674 Plates, *Iranian Journal of Science and Technology, Transactions of Civil Engineering*. 41 (2017) 13–
675 26. <https://doi.org/10.1007/s40996-016-0027-y>.
- 676 [23] FEMA 440 (ATC-55), Improvement of nonlinear static seismic analysis procedures, (2005).
- 677 [24] ASCE/SEI 41-17, Seismic Evaluation and Retrofit of Existing Buildings, 2017.
678 <https://doi.org/10.1061/9780784414859>.
- 679 [25] ACI 318, Building Code Requirements for Structural Concrete and Commentary, 2014.
680 [https://www.concrete.org/store/productdetail.aspx?ItemID=31814&Format=PROTECTED_PDF&Langu](https://www.concrete.org/store/productdetail.aspx?ItemID=31814&Format=PROTECTED_PDF&Language=English&Units=US_Units)
681 [age=English&Units=US_Units](https://www.concrete.org/store/productdetail.aspx?ItemID=31814&Format=PROTECTED_PDF&Language=English&Units=US_Units) (accessed February 14, 2019).
- 682 [26] AISC 360, Specification for Structural Steel Buildings, (2016). [https://www.aisc.org/Specification-for-](https://www.aisc.org/Specification-for-Structural-Steel-Buildings-ANSIAISC-360-16-1#.XGXrjlxKjIU)
683 [Structural-Steel-Buildings-ANSIAISC-360-16-1#.XGXrjlxKjIU](https://www.aisc.org/Specification-for-Structural-Steel-Buildings-ANSIAISC-360-16-1#.XGXrjlxKjIU) (accessed February 14, 2019).
- 684 [27] G.G. Meyerhof, The ultimate bearing capacity of foundations, *Géotechnique*. 2 (1951) 301–332.
685 <https://doi.org/10.1680/geot.1951.2.4.301>.
- 686 [28] K. Terzaghi, R.B. Peck, G. Mesri, *Soil mechanics in engineering practice*, John Wiley & Sons, 1996.
- 687 [29] B. Benmokrane, B. Zhang, A. Chenouf, Tensile properties and pullout behaviour of AFRP and CFRP
688 rods for grouted anchor applications, *Construction and Building Materials*. 14 (2000) 157–170.
689 [https://doi.org/10.1016/S0950-0618\(00\)00017-9](https://doi.org/10.1016/S0950-0618(00)00017-9).
- 690 [30] J. Mander, M. Priestley, Park, Theoretical stress–strain model for confined concrete, *American Society*
691 *of Civil Engineers*. 114 (1988) 1804–1826.
- 692 [31] J.E. Martínez-Rueda, A.S. Elnashai, Confined concrete model under cyclic load, *Materials and Struc-*
693 *tures*. 30 (1997) 139–147. <https://doi.org/10.1007/BF02486385>.
- 694 [32] S. Elkholy, B.E. Ariss, Enhanced external progressive collapse mitigation scheme for RC structures,
695 *International Journal of Structural Engineering*. 7 (2016) 63.
696 <https://doi.org/10.1504/IJSTRUCTE.2016.073679>.
- 697 [33] Charney Finley A., *Seismic Loads: Guide to the Seismic Load Provisions of ASCE 7-10*, 2015.
698 <https://doi.org/10.1061/9780784413524>.
- 699 [34] Computer and Structures Inc, *Concrete Frame Design Manual ACI 318-11 for SAP 2000*, (2016).
700 <http://docs.csiamerica.com/manuals/sap2000/Design/CFD-ACI-318-11.pdf> (accessed February 9,
701 2019).
- 702 [35] D. Saborio-Romano, G.J. O'Reilly, D.P. Welch, L. Landi, Simplified Pushover Analysis of Moment Re-
703 sisting Frame Structures AU - Sullivan, Timothy J., *Journal of Earthquake Engineering*. (2018) 1–28.
704 <https://doi.org/10.1080/13632469.2018.1528911>.

- 705 [36] R. Sheth, J. Prajapati, D. Soni, Comparative study nonlinear static pushover analysis and displacement
706 based adaptive pushover analysis method, *International Journal of Structural Engineering*. 9 (2018)
707 81–90. <https://doi.org/10.1504/IJSTRUCTE.2018.090753>.
- 708 [37] Azarbakht Alireza, Dolšek Matjaž, Progressive Incremental Dynamic Analysis for First-Mode Dominat-
709 ed Structures, *Journal of Structural Engineering*. 137 (2011) 445–455.
710 [https://doi.org/10.1061/\(ASCE\)ST.1943-541X.0000282](https://doi.org/10.1061/(ASCE)ST.1943-541X.0000282).
- 711 [38] S.W. Han, A.K. Chopra, Approximate incremental dynamic analysis using the modal pushover analysis
712 procedure, *Earthquake Engineering & Structural Dynamics*. 35 (2006) 1853–1873.
713 <https://doi.org/10.1002/eqe.605>.
- 714 [39] D. Vamvatsikos, Performing incremental dynamic analysis in parallel, *Computers & Structures*. 89
715 (2011) 170–180. <https://doi.org/10.1016/j.compstruc.2010.08.014>.
- 716 [40] Cimellaro G. P., Giovine T., Lopez-Garcia D., Bidirectional Pushover Analysis of Irregular Structures,
717 *Journal of Structural Engineering*. 140 (2014) 04014059. [https://doi.org/10.1061/\(ASCE\)ST.1943-541X.0001032](https://doi.org/10.1061/(ASCE)ST.1943-541X.0001032).
- 718 [41] Q.-S. “Kent” Yu, R. Pugliesi, M. Allen, C. Bischoff, Assessment of modal pushover analysis procedure
719 and its application to seismic evaluation of existing buildings, in: *13th World Conference on Earthquake*
720 *Engineering*, Vancouver, Canadá, 2004: p. Paper No. 1104.
- 721 [42] T.Y.P. Yuen, J.S. Kuang, D.Y.B. Ho, Ductility design of RC columns. Part 1: consideration of axial
722 compression ratio, *HKIE Transactions*. 23 (2016) 230–244.
723 <https://doi.org/10.1080/1023697X.2016.1232179>.
- 724 [43] AIS, NSR-10. Reglamento Colombiano de Construcción Sismo Resistente, Bogotá, DC. (2010).
- 725 [44] A. Neville, Core Tests: Easy to perform, Not easy to interpret, *Concrete International*. 23 (2001) 59–68.
726
727

Cartagena, October 17th, 2019

Highlights:

- Steel jacketing enhances existing RC columns axial and flexural strength
- Stiffening joints of RC buildings increases frame lateral loads capacity
- Inelastic behavior of retrofitted RC buildings suffers a significant improvement
- Structural irregularities and codes non-compliances affect the seismic performance

Sincerely yours,



Sergio Villar S.
cc. 93194496 of 9na

Sergio Villar Salinas, MsC

Professor

Department of Civil and Environmental Engineering

Universidad Tecnológica de Bolívar

Campus Tecnológico Km 1. Vía Turbaco

Cartagena de Indias, BOL, Colombia 130010

svillars@utb.edu.co

www.utb.edu.co

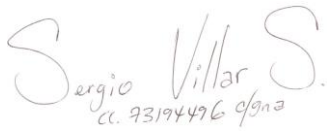
Phone: [575] 3008038640

Cartagena, December 10th, 2019

Conflict of interest:

The authors declare that they have no known competing financial interests or personal relationships that could have appeared to influence the work reported in this paper.

Sincerely yours,



Sergio Villar S.
C.C. 93194496 of 9na

Sergio Villar Salinas, MSc

Professor

Department of Civil and Environmental Engineering

Universidad Tecnológica de Bolívar

Campus Tecnológico Km 1. Vía Turbaco

Cartagena de Indias, BOL, Colombia 130010

svillars@utb.edu.co

www.utb.edu.co

Phone: [575] 3008038640